ACS APPLIED MATERIALS & INTERFACES

Research Article

www.acsami.org

TiO_2 Nanotubes: Interdependence of Substrate Grain Orientation and Growth Rate

Silvia Leonardi,[†] Valeria Russo,[‡] Andrea Li Bassi,[‡] Fabio Di Fonzo,[§] Thomas M. Murray,[∥] Harry Efstathiadis,[∥] Andrea Agnoli,[⊥] and Julia Kunze-Liebhäuser*[,†,#]

[†]Department of Physics E19 and Institute for Advanced Study, Technische Universität München, James-Franck-Strasse 1, 85748 Garching, Germany

[‡]Department of Energy and NEMAS (Center for NanoEngineered MAterials and Surfaces), Politecnico di Milano, via Ponzio 34/3, 20133 Milan, Italy

[§]Center for Nano Science and Technology@PoliMi, Istituto Italiano di Tecnologia, via Pascoli 70/3, 20133 Milan, Italy

[∥]Colleges of Nanoscale Science and Engineering, State University of New York Polytechnic Institute, 257 Fuller Road, Albany, New York 12203, United States

[⊥]MINES ParisTech, Center for Materials Forming (CEMEF), UMR CNRS 7635, BP 207, 06904 Sophia-Antipolis, France

[#]Institute of Physical Chemistry, University of Innsbruck, Innrain 52c, 6020 Innsbruck, Austria

Supporting Information

ABSTRACT: Highly ordered arrays of TiO_2 nanotubes can be produced by self-organized anodic growth. It is desirable to identify key parameters playing a role in the maximization of the surface area, growth rate, and nanotube lengths. In this work, the role of the crystallographic orientation of the underlying Ti substrate on the growth rate of anodic self-organized TiO_2 nanotubes in viscous organic electrolytes in the presence of small amounts of fluorides is studied. A systematic analysis of cross sections of the nanotubular oxide films on differently oriented substrate grains was conducted by a combination of electron backscatter diffraction and scanning electron microscopy. The characterization allows for a correlation between TiO_2 nanotube lengths and diameters and crystallographic parameters of the underlying Ti metal substrate, such as planar surface densities. It is found that the growth rate of TiO_2 nanotubes gradually increases with the decreasing planar atomic density of the titanium substrate. Anodic TiO_2 nanotubes with the highest aspect ratio form on Ti(−151) [which is close to Ti(010)], whereas nanotube formation is completely inhibited on Ti(001). In the thin compact oxide on Ti(001), the electron donor concentration and electronic conductivity are higher, which leads to a competition between oxide growth and other electrochemical oxidation reactions, such as the oxygen evolution reaction, upon anodic polarization. At grain boundaries between oxide films on Ti(*hk*0), where nanotubes grow, and Ti(001), where thin compact oxide films are formed, the length of nanotubes decreases most likely because of lateral electron migration from TiO_2 on Ti(001) to TiO_2 on Ti(*hk*0).

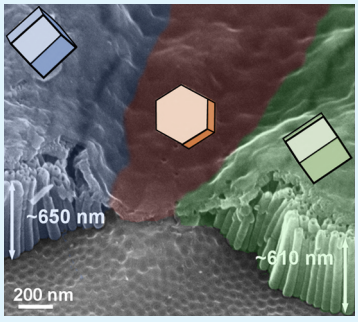

KEYWORDS: *anodic TiO_2 nanotubes, EBSD, self-organized anodic growth, growth rate, organic electrolyte*

INTRODUCTION

Since the first report of anodic self-organized Al_2O_3 pore formation on Al substrates,[1] anodic self-organized oxide nanostructures grown on valve metals have been intensely investigated. Anodic oxide films grown on valve metals have no or very low electronic conductivity, so that besides the ionic current responsible for oxide film growth, almost no electronic current, associated with side reactions, such as the oxygen evolution reaction, taking place at the surface of the oxide film, can flow through the film. Self-organized anodic TiO_2 nanotube arrays[2−4] are highly interesting materials among valve metal oxides, because of the combination of a regular and controllable nanoscale geometry with the various functional properties of titania, which make the material suitable for applications in, e.g., electrocatalysis[5,6] and photocatalysis,[7] solar energy conversion,[8,9] sensing,[10] biomedical devices,[11,12] and Li-ion batteries.[13−15] A large variety of nanotube morphologies can be obtained by fine-tuning the electrochemical anodization parameters. Effects of applied potential, anodization time, solution composition, and pH on the resulting oxide properties have been reported.[16] The proposed growth mechanisms for TiO_2 nanotube formation refer to a combination of flow and dissolution models.[17,18] Self-organized anodic processes in highly viscous electrolytes can lead to the formation of high-aspect-ratio nanotubular TiO_2 arrays.[16] In this regard, it is desirable to identify the key parameters playing a role in the

Received: October 17, 2014
Accepted: December 29, 2014
Published: December 29, 2014

DOI: 10.1021/am507181p
ACS Appl. Mater. Interfaces 2015, 7, 1662−1668

maximization of the surface area, overall growth rate, and nanotube lengths.

Nanotubular anodic TiO_2 growth in fluoride-containing electrolytes has been extensively investigated since its discovery in 1999.[2] Compact anodic TiO_2, formed in fluoride-free electrolytes, has also been thoroughly studied for a long time (see ref 29 for a review). In the case of compact anodic TiO_2 grown on Ti, it has been shown that the TiO_2 film thickness, donor concentration, and electronic conductivity depend on the crystallographic orientation of the Ti substrate grains, and that the rate of ion transfer reactions (e.g., passive film growth) and electron transfer reactions (e.g., oxygen evolution) differ from grain to grain.[19−23] A combination of electrochemical analysis with high spatial resolution and electron backscatter diffraction (EBSD) has been employed to study the correlation between the crystallographic orientation of the underlying Ti metal substrate and the electrochemical behavior of the compact anodic oxide formed on top.[22] The layer thickness and crystallinity of anodic compact TiO_2 were analyzed. It was found that thin crystalline, electronically conductive oxide films are formed on Ti(001), whereas thicker less crystalline films with lower electronic conductivity grow on Ti(*hk*0). A direct consequence of the significant electron conductivity of the growing anodic TiO_2 films is that, besides the ionic current responsible for film growth, an electronic current, associated with side reactions taking place at the surface of the oxide film, can flow through the film. Therefore, there is a competition between oxide growth and other electrochemical oxidation side reactions, being mainly the oxygen evolution reaction.[29] For TiO_2 on Ti(001), anodic oxygen evolution takes place at potentials of >4 V, whereas on Ti(*hk*0) and misoriented grains, oxide formation is the only charge transfer reaction observed, which leads to the formation of thick passive films.[22]

In an earlier paper, the authors showed how the growth characteristics of anodic nanotubular TiO_2 films, produced in an aqueous electrolyte solution of 1 M $(NH_4)H_2PO_3$ and 0.5 wt % NH_4F, can be tailored by controlling the orientation of the underlying Ti metal substrate.[24] It was found that open or partially capped amorphous TiO_2 nanotubes form on Ti(*hk*0) grains, where growth of thick nanotubular oxide films was permitted. On Ti(001) grains, no open nanotubes but compact oxide films were observed, exhibiting a mixed anatase and rutile nanocrystalline character with a large degree of structural disorder.[24,30] Except for this study,[24] only one paper describes retarded nanotube growth on the Ti(001) surface.[31] The results reported therein, even though interesting, do not provide a detailed understanding of the interdependence of nanotube growth and grain structure, resulting in deriving only qualitative conclusions.

In this work, we report on the anodization of polycrystalline Ti metal surfaces in glycerol-based electrolytes with small additions of fluorides and on the analysis of the growth rates of anodic titania nanotubes on differently oriented Ti substrate grains. The organic electrolyte with small amounts of fluorides was chosen to optimize the conversion efficiency by decreasing the oxide dissolution rate and, at the same time, to fabricate nanotubes with a more defined ripple-free geometry, as previously shown in studies of the nanotube growth mechanism.[18] The cross section analysis of TiO_2 nanotubes allowed the characterization of their length as a function of the crystallographic orientation and the corresponding planar atomic densities of the underlying Ti metal substrate and provided information about the growth mechanism.

EXPERIMENTAL SECTION

Reagents, Solutions, and Electrode Materials. TiO_2 nanotubes have been grown on 1 mm thick polycrystalline Ti sheets (99.96% pure, AdventMaterials Ltd.) with an edge length of 1 cm. Prior to the anodic treatment, each Ti substrate was mechanically polished by using wet SiC grinding paper (grade 4000) followed by an electropolishing step in a mixture of methanol (≥99.9% pure, Merck), perchloric acid ($HClO_4$, 40%) (99.9% suprapure, Merck), and butoxyethanol (≥99% pure, Alfa Aesar).[25] For electropolishing, the Ti substrates were wrapped in Teflon tape with an opening providing an exposed area of ∼80 mm^2 during the electropolishing treatment. A potential of 60 V was applied for 5 min between the sample and a gold counter electrode. The electropolishing solution was held between −20 and −40 °C during the entire growth process. At the end of each electropolishing treatment, all substrates were cleaned in ethanol (absolute grade emsure, VWR Chemicals) in an ultrasonic bath (Sonorex, Bandelin Electronic) and rinsed with Milli-Q [deionized (DI)] water (resistivity of 18.2 MΩ cm at 25 °C, Millipore). After two electropolishing cycles, the Teflon mask was removed and the samples were sonicated for 30 min in ethanol (99.9% empure, VWR Chemicals) before being rinsed with DI water. Prior to the anodization treatment, the Ti substrates were further degreased by sonication in acetone, 2-propanol, and methanol, thoroughly rinsed with DI water, and finally dried in a nitrogen stream. Anodic growth of all TiO_2 nanotube arrays presented in this paper was conducted in a mixed electrolyte solution of glycerol (anhydrous, ≥99.95% pure, Merck) and 0.25 wt % NH_4F (99.998% pure, Merck). All chemicals were used without further purification.

Electrochemical Synthesis and Instrumentation. A conventional two-electrode Teflon electrochemical cell with a platinum gauze as a counter electrode was employed for the synthesis of the TiO_2 nanotubes. Prior to each experiment, the cell was cleaned in Caro's acid (3:1 mixture of H_2SO_4 and H_2O_2) and thoroughly rinsed with DI water. Nanotube growth was conducted at room temperature without stirring at a constant voltage of 20 V for 6 h by using a DC power supply (PS240 3D, Fluke). The final potential was reached by ramping from 0 to 20 V with a rate of ∼1 V s^{-1}. After anodic nanotube production, each sample was thoroughly rinsed with DI water and dried in a nitrogen stream.

Surface Analysis. *Electron Backscatter Diffraction (EBSD).* The inverse pole figure (IPF) of polycrystalline Ti and the related grain orientation map was obtained on a defined area of the metal substrates by EBSD. The IPF represents the stereographic projection leading to 32 crystallographic classes in six systems and shows the grain orientations characterizing the surface texture of the titanium substrate. The IPF shows how the selected direction in the sample reference frame is distributed in the reference frame of the crystal. The directions plotted are the stereographic projection of crystal directions parallel to the normal direction (ND), rolling direction (RD), or transverse direction (TD) in the sample. During the measurement, an amorphous ∼1.3−5.4 nm thick native oxide was considered,[26] which is thin compared to the information depth of ∼20 nm[22] of EBSD and therefore does not lead to a decrease in pattern quality due to scattering. The area for the map was indicated by fiducial marks milled into the sample using a Ga beam with an accelerating voltage of 30 kV and a beam current of 21 nA. During milling, the surface was sealed with ink from a Sharpie pen to avoid contamination. After milling, the ink was removed by sonicating the sample in acetone followed by ethanol. The standard measurement configuration (45° pretilted specimen mount, Ted Pella catalog no. 16355, 70° angle between the electron beam and surface) with tilt correction was used to record a microstructural map of 50 μm × 50 μm with a step size of 0.5 μm. A field emission scanning electron microscope (FEI Nova NanoSEM600 Dualbeam, HKL Channel 5), with an acceleration voltage of 30 kV, a working distance of 12−15 mm, and a beam current of 0.64 nA, was used to collect the EBSD pattern. A set of three Euler angles (φ_1, Φ, and φ_2) is generally retrieved from EBSD analysis to fully determine the crystallographic orientation of grains in a three-dimensional system. To describe the crystallographic texture in hcp systems, like Ti,

DOI: 10.1021/am507181p
ACS Appl. Mater. Interfaces 2015, 7, 1662−1668

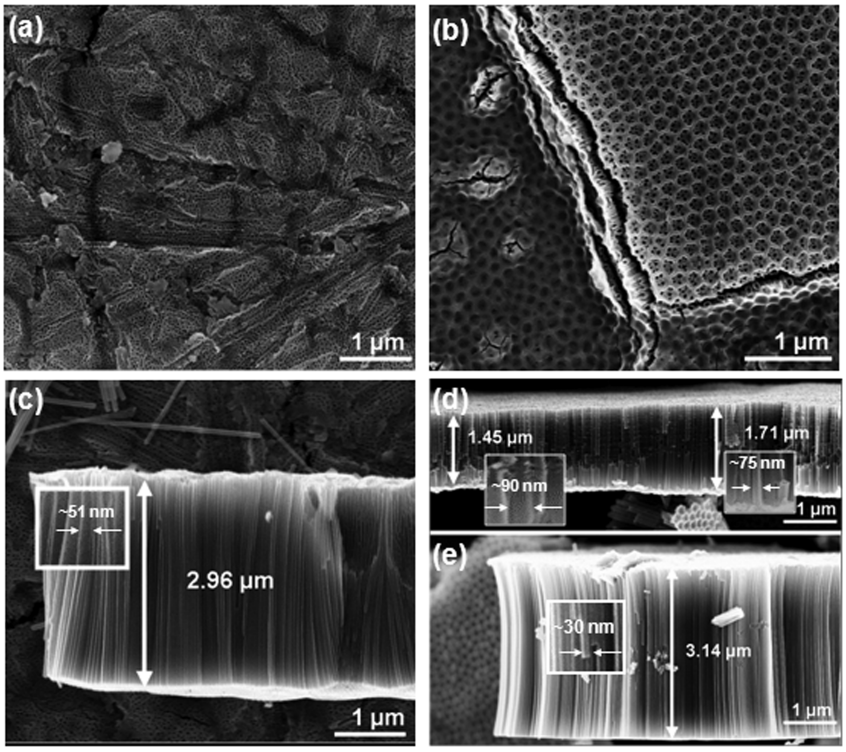

Figure 1. SEM top views and cross sections of TiO_2 nanotubes grown in glycerol with 0.25 wt % NH_4F at 20 V for 6 h on nonelectropolished (a and c) and electropolished (b, d, and e) Ti substrates. In panel d, the nanotube layer is flipped upside down, and the nanotube bottoms show ripples (see the left inset in panel d).

either Miller-Bravais Indices {*hkil*} or Miller indices {*hkl*} were used. The transformation from Euler space to the (*hkil*) planes was obtained by applying a simple matrix multiplication.[22,27] Planar surface densities were calculated for the differently oriented Ti substrate surfaces using a modeling tool enclosed in CrystalKit.

Scanning Electron Microscopy (SEM). All SEM analysis was conducted with a Zeiss Supra 40 field emission microscope. Cross section images of specific grains were acquired by tilting the specimen mount to a 45° angle between the surface normal and the microscope detector. The tilt was then corrected to determine the real nanotube lengths. For cross section SEM imaging, a homemade setup consisting of tungsten needles with tip dimensions of 10 μm in diameter mounted on micro manipulators (Wenthwort, model PVX-400) and equipped with an optical microscope was used to scratch through grains on the anodized surface inside the area previously mapped with EBSD.

RESULTS AND DISCUSSION

Figure 1 shows SEM micrographs of TiO_2 nanotubes grown on nonelectropolished and electropolished Ti substrates. The TiO_2 nanotube array formed on the nonelectropolished Ti substrate is covered by a disordered capping layer (Figure 1a), which is typically observed for organic electrolytes.[28] The crystallographic structure of the underlying metal substrate has no influence on the nanotube growth rate. Upon statistical analysis of cross sections taken on different areas, it is observed that the nanotubes have the same average length of ~3 μm all over the surface (Figure 1c). Their length depends on the fluoride concentration and on the anodization time, as reported previously.[16] The outer nanotube diameter and the side wall thickness, both measured at the nanotube top, are ~50 and ~4 nm, respectively (see Figure 1c and Figure S1a of the Supporting Information). The walls have a completely smooth morphology from top to bottom (see Figure S1 of the Supporting Information). On electropolished substrates, a grain structure is clearly visible and the capping layer that covers the topmost nanotube surface shows a different morphology on different substrate grains (Figure 1b). At least four zones with different growth rates are identified (see Figure S2 of the Supporting Information) in which nanotube lengths range from ~1.5 to ~3.1 μm (see Figure 1d,e). The nanotube outer diameters range from ~30 to ~90 nm, where the longest nanotubes (3.1 μm) have the smallest diameter of ~30 nm and the shorter nanotubes (1.5 and 1.7 μm) have diameters of ~90 and 75 nm, respectively. The morphology of the tube walls is mainly smooth, but on some grains, ripples are observed at the nanotube bottoms that form at later growth stages (Figure 1d).

To gain a better understanding of the factors that lead to the formation of high-aspect-ratio TiO_2 nanotubes in organic electrolytes and, in particular, the role the substrate grain orientations play, the Ti metal substrate was characterized by EBSD after electropolishing and prior to anodization. The inverse pole figure (IPF) of the Ti metal substrate, detected with EBSD, is depicted in Figure 2. Crystallographic orientations of the planes characterizing the Ti substrate texture are given by the color legend of the corresponding orientation distribution map (Figure 2). To evaluate the growth rate dependence of TiO_2 nanotubes on the orientation of the underlying substrate (see Figure 1), cross sections of TiO_2 nanotubes grown on differently oriented substrate grains were taken to correlate nanotube length and substrate orientation. The positions where cross sections were analyzed are indicated on the EBSD map in Figure 2.

Figure 3 shows a SEM cross section through TiO_2 nanotubes formed on substrate grains identified as Ti(−160), Ti(001), and Ti(−120) planes. These orientations correspond to the light blue, red, and green areas of the map, respectively (Figure

DOI: 10.1021/am507181p
ACS Appl. Mater. Interfaces 2015, 7, 1662−1668

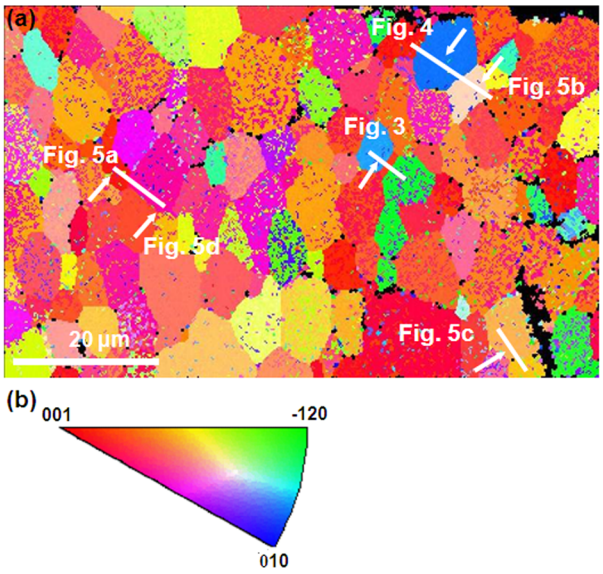

Figure 2. (a) Inverse pole figure (IPF) map of the area where cross sections of the nanotubular film are investigated with SEM. Cross sections are marked by white lines. (b) Color legend for the IPF explaining the crystallographic orientations (orientations of the vertices refer to substrate planes).

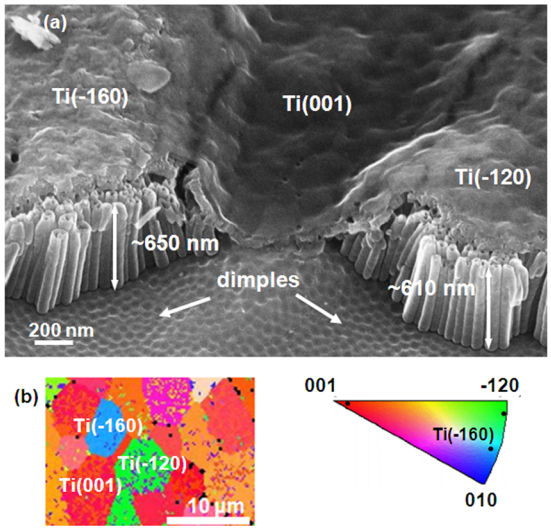

Figure 3. (a) Cross section of anodic TiO_2 nanotubes grown in glycerol with 0.25 wt % NH_4F at 20 V for 6 h on Ti(−160)-, Ti(001)-, and Ti(−120)-oriented grains. (b) EBSD map and stereographic triangle showing the positions of substrate grains underlying the nanotubular oxides.

3b). Anodization of titanium metal grains with Ti(−160) and Ti(−120) orientations leads to the formation of ∼650 and ∼610 nm long TiO_2 nanotubes, whereas on the low-index plane Ti(001) (red area in the color legend), an 80 nm thick compact oxide film with no trace of porosity, chemical etching, or self-organized nanotube formation is grown. A pronounced grain boundary effect can be noticed where nanotube lengths on Ti(−160)- and Ti(−120)-oriented grains dramatically decrease close to the compact oxide layer formed on Ti(001).

Figure 4 depicts a SEM cross section of nanotubular anodic oxide formed on a Ti(−151)-oriented grain, located in the blue area of the orientation distribution map, where the TiO_2 nanotube length reaches a value of ∼920 nm. This indicates

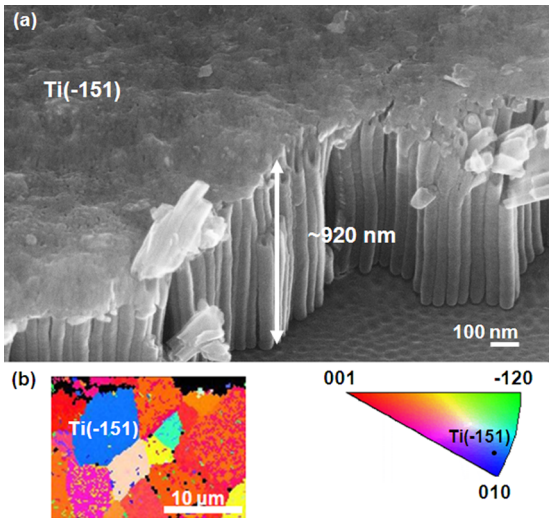

Figure 4. (a) SEM cross section of anodic TiO_2 nanotubes grown in glycerol with 0.25 wt % NH_4F at 20 V for 6 h on a Ti(−151)-oriented grain. (b) EBSD map and stereographic triangle showing the position of the substrate grain underlying the nanotubular oxide.

that the nanotube growth rate is enhanced on substrate orientations such as Ti(−151), when compared to that on Ti(001). It is important to note that, in this study, the nanotube lengths measured on the surface that was mapped with EBSD prior to nanotube growth were smaller than the lengths of nanotubes grown on Ti metal substrates right after electropolishing under the same growth conditions. This effect is most likely due to the treatment of the surface during milling with the Ga beam.

Analysis of the thickness of the titania nanotube films on different substrate grain orientations in the mapped area allows correlation of the substrate grain orientation with the growth rate. Figure 5 depicts SEM micrographs of six different grains from the IPF and the corresponding positions in the stereographic triangle. Clearly, different nanotube lengths are measured for the different substrate grain orientations. It is observed that short nanotubes of only 175 nm length covered with a thick compact capping layer are grown on approximately Ti(001)-oriented substrate grains, such as on Ti(017) (Figure 5a). On Ti(134)- and Ti(115)-oriented grains, nanotube lengths reach values of 290 and ∼330 nm, respectively (Figure 5b).

On Ti(−135) and Ti(114), the growth rate is increased, and nanotube lengths of ∼450 and 550 nm are obtained (Figure 5c). A further increase in growth rate is observed for nanotubes grown on Ti(01−3)-oriented grains, where 585 nm thick nanotubular films are formed (Figure 5d). As the thickness of the nanotube films increases, the thickness of the topmost capping layer decreases from ∼60 nm on Ti(017) to less than ∼20 nm on Ti(01−3).

In Figure 6, all nanotube lengths measured on differently oriented substrate grains are summarized. Figure 6 shows that nanotube growth rates are lowest on approximately (001)-oriented Ti substrate grains. The growth rate increases when the substrate grain orientation is changed by moving along the upper and lower edges of the stereographic triangle [with higher growth rates observed for the lower edge (black and blue curves in Figure 6a)]. Growth rates are considerably higher on grains with orientations belonging to the triangle edge connecting the Ti(−120) and Ti(010) vertices, where nano-

DOI: 10.1021/am507181p
ACS Appl. Mater. Interfaces 2015, 7, 1662−1668

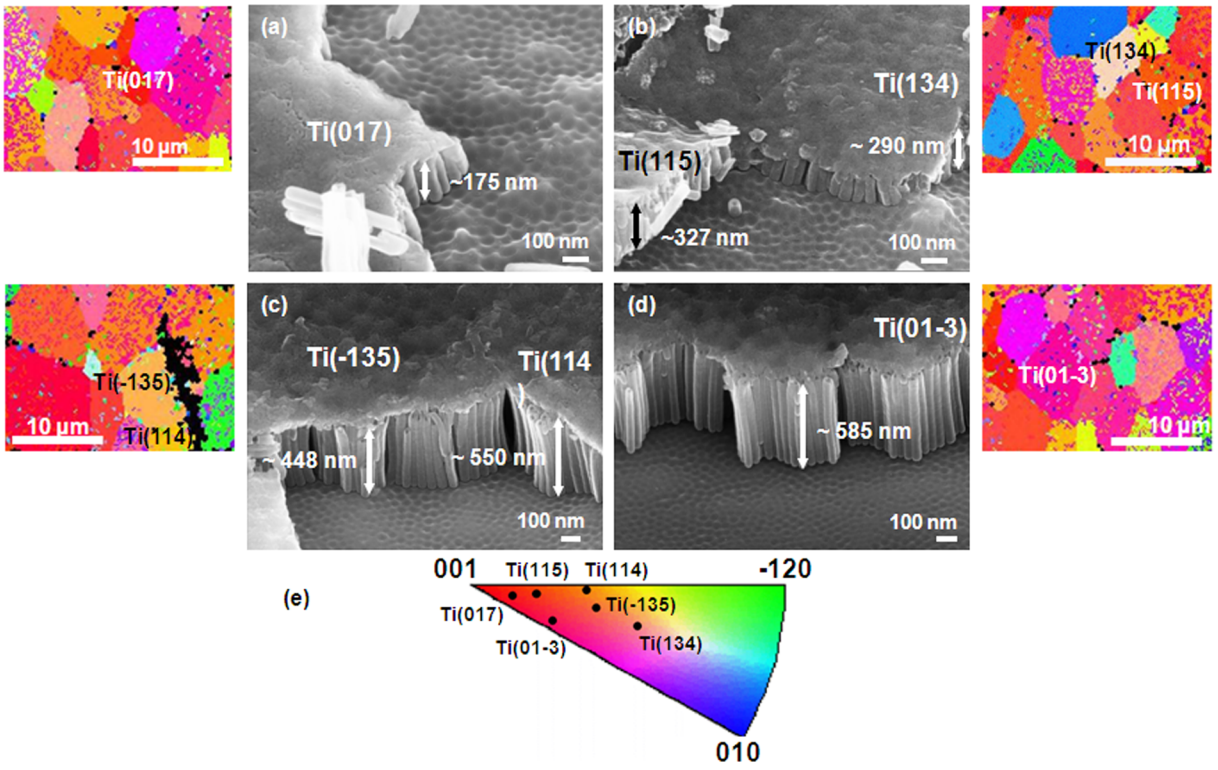

Figure 5. SEM cross sections of TiO_2 nanotubes grown in glycerol with 0.25 wt % NH_4F at 20 V for 6 h on differently oriented grains: (a) Ti(017), (b) Ti(115) and Ti(134), (c) Ti(−135) and Ti(114), and (d) Ti(01−3) with the corresponding IPF maps. (e) Stereographic triangle showing the positions of substrate grains underlying the nanotubular oxides.

tube lengths are never shorter than ~600 nm (blue line in Figure 6b). When substrate grain orientations change following a virtual line through the center of the stereographic triangle (black line in Figure 6b), the trend is not continuous because a lower growth rate is observed for TiO_2 nanotubes grown on Ti(134).

The correlation of Ti substrate grain orientation and its corresponding atomic planar density calculated as the number of atoms per surface area with TiO_2 nanotube length shows higher nanotube growth rates for lower planar atomic densities (Figure 7). It is known that TiO_2 nanotube growth starts with the formation of a compact oxide layer that is first chemically etched by the fluorides in the electrolyte, leading to the formation of an unordered porous oxide layer. After this initial phase, a self-organized growth of TiO_2 nanotubes takes place.[28] Consequently, the nature of the compact oxide film formed prior to nanotube formation plays an important role in self-organized nanotube growth. As mentioned in the Introduction, compact anodic oxide grown on Ti(001) is characterized by the highest electronic conductivity, which leads to enhanced oxygen evolution at the expense of oxide layer formation.[22,29] Our findings demonstrate that no TiO_2 nanotube growth takes place on Ti(001) substrate surfaces, which confirms our previous studies.[24]

It is important to note that a total absence of nanotubular features in the anodic film is observed only on a small portion of the Ti(001) grain narrowed between nanotube films on Ti(−160) and Ti(−120), whereas on a wider region of the same grain, dimples have formed. These dimples originate from TiO_2 nanotubes formed at the metal−oxide interface during the anodic self-organization process that were mechanically removed from the surface upon preparation of the cross section (see arrows in Figure 3). A possible explanation for this finding could be the limited lateral resolution of the EBSD map; the system is very sensitive to small changes in the crystallographic orientation, which might lead to nanotube growth on approximately (001)-oriented substrate grains (see, e.g., Figure 5a).

The pronounced grain boundary effect, where nanotube lengths on Ti(−160)- and Ti(−120)-oriented grains decrease at the boundary with the compact oxide layer formed on Ti(001), can be explained by a change in the electronic properties of TiO_2 grown on differently oriented substrate grains. Davepon et al.[23] provided evidence that the electron concentration in the oxide film formed on a given grain is not homogeneous but exhibits gradients across grain boundaries, if the film grown on an adjacent grain has a significantly different conductivity. According to these authors, this observation is proof for lateral electron migration across the oxide. For the case of decreasing TiO_2 nanotube length at grain boundaries with compact TiO_2 on Ti(001), lateral electron migration can occur from TiO_2 grown on Ti(001) to TiO_2 grown on Ti(hk0), leading to an increased electronic conductivity of TiO_2, and thus to a decrease in oxide growth rate, at the grain boundary.

CONCLUSIONS

Electron backscatter diffraction and scanning electron microscopy were used to investigate the growth rate of anodic, self-organized nanotubular titania in organic electrolytes and its dependence on the crystallographic orientations of the underlying Ti substrate grains. It was found that TiO_2 nanotubes with the highest aspect ratio are formed on Ti(−151), whereas compact TiO_2 films grow on Ti(001). It was observed that the growth rate of TiO_2 nanotubes gradually

DOI: 10.1021/am507181p
ACS Appl. Mater. Interfaces 2015, 7, 1662−1668

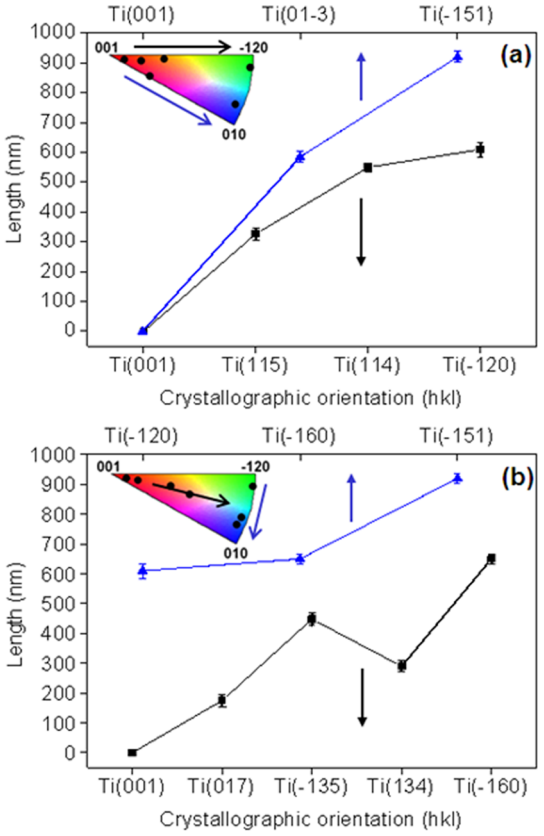

Figure 6. TiO_2 nanotube lengths for anodic films grown in glycerol with 0.25 wt % NH_4F for 6 h at 20 V on differently oriented substrate grains (standard deviations refer to length variations inside the same substrate grain). Changes of plane orientations (a) along upper (black curve) and lower (blue curve) edges of the stereographic triangle and (b) from (−120) to (010) (blue curve) and through the high-index inner planes (black curve) of the stereographic triangle.

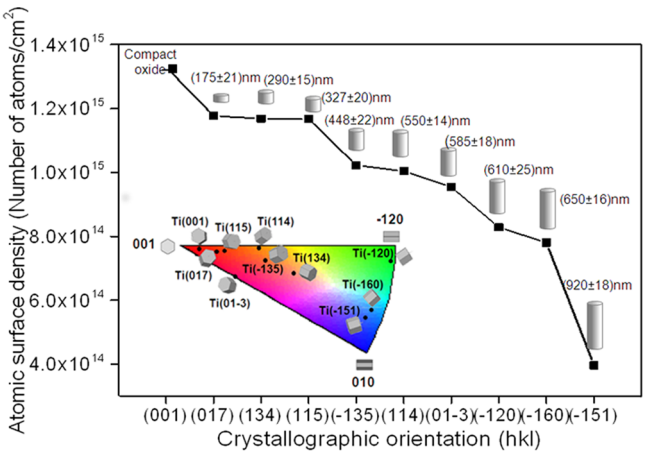

Figure 7. Atomic surface densities of Ti metal substrate planes and their correlation with TiO_2 nanotube lengths (standard deviations refer to length variations inside the same grain). Connecting lines are inserted as a guide for the eye. The inset shows the orientation of hexagonal 3D unit cells of Ti substrate grains determined from Euler angles obtained with EBSD.

increases with the decreasing planar atomic density of the titanium substrate. TiO_2 nanotube length decreases at grain boundaries between compact oxide films formed on Ti(001) and nanotube-forming films on Ti(*hk*0) because of lateral electron migration from TiO_2 with a higher electron concentration present on Ti(001) to TiO_2 with a lower electron concentration present on Ti(*hk*0).

■ ASSOCIATED CONTENT

Supporting Information

Details of TiO_2 nanotube morphology (Figure S1) and image of the capping layer that covers the topmost nanotube surface that shows a different morphology on differently oriented substrate grains on electropolished substrates (Figure S2). This material is available free of charge via the Internet at http://pubs.acs.org.

■ AUTHOR INFORMATION

Corresponding Author

*E-mail: julia.kunze@uibk.ac.at.

Funding

We thank the DFG (Project KU 2397/1-1) and the Technische Universität München (TUM) Institute for Advanced Study, funded by the German Excellence Initiative, for financial support.

Notes

The authors declare no competing financial interest.

■ ACKNOWLEDGMENTS

We thank Dr. Alessandro Luzio of the Italian Institute of Technology for providing the setup and expertise in cross section preparation.

■ REFERENCES

(1) Masuda, H.; Fukuda, K. Ordered Metal Nanohole Arrays Made by a Two-Step Replication of Honeycomb Structures of Anodic Alumina. *Science* **1995**, *268*, 1466−1468.

(2) Zwilling, V.; Darque-Ceretti, E.; Boutry-Forveille, A.; David, D.; Perrin, M. Y.; Aucouturier, M. Structure and Physicochemistry of Anodic Oxide Films on Titanium and TA6V Alloy. *Surf. Interface Anal.* **1999**, *27*, 629−637.

(3) Zwilling, V.; Aucouturier, M.; Darque-Ceretti, E. Anodic Oxidation of Titanium and TA6V Alloy in Chromic Media. An Electrochemical Approach. *Electrochim. Acta* **1999**, *45*, 921−929.

(4) Beranek, R.; Hildebrand, H.; Schmuki, P. Self-Organized Porous Titanium Oxide Prepared in H_2SO_4/HF Electrolytes. *Electrochem. Solid-State Lett.* **2003**, *6*, B12−B14.

(5) Macak, J. M.; Tsuchiya, H.; Bauer, S.; Schmuki, P.; Barczuk, P.; Nowakoska, M. Z.; Chojak, M.; Kulesza, P. J. Self-organized Nanotubular TiO_2 Matrix as Support for Dispersed Pt/Ru Nanoparticles, Enhancement of the Electrocatalytic Oxidation of Methanol. *Electrochem. Commun.* **2005**, *7*, 1417−1422.

(6) Hahn, R.; Ghicov, A.; Tsuchiya, H.; Macak, J. M.; Muñoz, A. G.; Schmuki, P. Lithium-Ion Insertion in Anodic TiO_2 Nanotubes Resulting in High Electrochromic Contrast. *Phys. Status Solidi A* **2007**, *204*, 1281−1285.

(7) Kontos, A. G.; Kontos, A. I.; Tsoukleris, D. S.; Likodimos, V.; Kunze, J.; Schmuki, P.; Falaras, P. Photo-Induced Effects on Self-organized TiO_2 Nanotube Arrays: The Influence of Surface Morphology. *Nanotechnology* **2009**, *20*, 045603.

(8) Ghicov, A.; Albu, S. P.; Hahn, R.; Kim, D.; Stergiopoulos, T.; Kunze, J.; Schiller, C.-A.; Falaras, P.; Schmuki, P. TiO_2 Nanotubes in Dye-Sensitized Solar Cells: Critical Factors for the Conversion Efficiency. *Chem.—Asian J.* **2009**, *4*, 520−525.

(9) Macak, J. M.; Tsuchiya; Ghicov, A.; Schmuki, P. Dye-sensitized Anodic TiO_2 Nanotubes. *Electrochem. Commun.* **2005**, *7*, 1133−1137.

(10) Varghese, O. K.; Gong, D.; Paulose, M.; Ong, K. G.; Grimes, C. A. Hydrogen Sensing Using Titania Nanotubes. *Sens. Actuators, B* **2003**, *93*, 338−344.

DOI: 10.1021/am507181p
ACS Appl. Mater. Interfaces 2015, 7, 1662−1668

(11) Tsuchiya, H.; Macak, J. M.; Müller, L.; Kunze, J.; Müller, F.; Greil, P.; Virtanen, S.; Schmuki, P. Hydroxyapatite Growth on Anodic TiO_2 Nanotubes. *J. Biomed. Mater. Res.* **2006**, *77A*, 534−541.
(12) Kunze, J.; Müller, L.; Macak, J. M.; Greil, P.; Schmuki, P.; Müller, F. A. Time-dependent Growth of Biomimetic Apatite on Anodic TiO_2 Nanotubes. *Electrochim. Acta* **2008**, *53*, 6995−7003.
(13) Brumbarov, J.; Kunze-Liebhäuser, J. Silicon on Conductive Self-organized TiO_2 Nanotubes: A High Capacity Anode Material for Li-ion batteries. *J. Power Sources* **2014**, *558*, 129−133.
(14) Wu, Q. L.; Li, J.; Deshpande, R. D.; Subramanian, N.; Rankin, S. E.; Yang, F.; Cheng, Y.-T. Aligned TiO_2 Nanotube Arrays as Durable Lithium-Ion Battery Netagive Electrodes. *J. Phys. Chem. C* **2012**, *116*, 18669−18677.
(15) Fang, H.-T.; Liu, M.; Wang, D.-W.; Sun, T.; Guan, D.-S.; Li, F.; Zhou, J.; Sham, T.-K.; Cheng, H.-M. Comparison of the Rate Capability of Nanostructured Amorphous and Anatase TiO_2 for Lithium Insertion Using Anodic TiO_2 Nanotube Arrays. *Nanotechnology* **2009**, *20*, 225701.
(16) Roy, P.; Berger, S.; Schmuki, P. TiO_2 Nanotubes: Synthesis and Applications. *Angew. Chem., Int. Ed.* **2011**, *50*, 2904−2939.
(17) Le Clere, D. J.; Valota, A.; Skeldon, P.; Thompson, G. E.; Berger, S.; Kunze, J.; Schmuki, P.; Habazaki, H.; Nagata, S. Tracer Investigation of Pore Formation in Anodic Titania. *J. Electrochem. Soc.* **2008**, *155*, C487−C494.
(18) Berger, S.; Macak, J. M.; Kunze, J.; Schmuki, P. High-efficiency Conversion of Sputtered Ti Thin Films into TiO_2 Nanotubular Layers. *Electrochem. Solid-State Lett.* **2008**, *11*, C37−C40.
(19) Schultze, J. W.; Kudelka, S. Microtechniques Open Doorways to a New Understanding of Electrochemical Systems. *Interface* **1997**, *6*, 28.
(20) Kudelka, S.; Schultze, J. W. Photoelectrochemical Imaging and Microscopic Reactivity of Oxidised Ti. *Electrochim. Acta* **1997**, *42*, 2817−2825.
(21) Kudelka, S.; Michaelis, A.; Schultze, J. W. Effect of Texture and Formation Rate on Ionic and Electronic Properties of Passive Layers on Ti Single Crystals. *Electrochim. Acta* **1996**, *41*, 863−870.
(22) König, U.; Davepon, B. Microstructure of Polycrystalline Ti and its Microelectrochemical Properties by Means of Electron-Backscattering Diffraction (EBSD). *Electrochim. Acta* **2001**, *47*, 149−160.
(23) Davepon, B.; Schultze, J. W.; König, U.; Rosenkranz, C. Crystallographic Orientation of Single Grains of Polycrystalline Titanium and Their Influence on Electrochemical Processes. *Surf. Coat. Technol.* **2003**, *169−170*, 85−90.
(24) Leonardi, S.; Li Bassi, A.; Russo, V.; Di Fonzo, F.; Paschos, O.; Murray, T. M.; Efstathiadis, H.; Kunze, J. TiO_2 Nanotubes: Interdependence of Substrate Grain Orientation and Growth Characteristics. *J. Phys. Chem. C* **2012**, *116*, 384−392.
(25) Arsov, L. D. Dissolution Electrochimique des Films Anodiques du Titane dans l'Acide Sulfurique. *Electrochim. Acta* **1985**, *30*, 1645−1657.
(26) Schultze, J. W.; Lohrengel, M. M. Stability, Reactivity and Breakdown of Passive Films. Problems of Recent and Future Research. *Electrochim. Acta* **2000**, *45*, 2499−2513.
(27) Kallend, J. S.; Kocks, U. F.; Rollett, A. D.; Wenk, H.-R. Operational Texture Analysis. *Mater. Sci. Eng., A* **1991**, *132*, 1−11.
(28) Berger, S.; Kunze, J.; Schmuki, P.; LeClere, D.; Valota, A.; Skeldon, P.; Thompson, G. A Lithographic Approach to Determine Volume Expansion Factors During Anodization: Using the Example of Initiation and Growth of TiO_2-Nanotubes. *Electrochim. Acta* **2009**, *54*, 5942−5948.
(29) Van Humbeek, J.-F.; Proost, J. Current Understanding of Ti Anodisation: Functional, Morphological, Chemical and Mechanical Aspects. *Corros. Rev.* **2009**, *27*, 117−204.
(30) Likodimos, V.; Stergiopoulos, T.; Falaras, P.; Kunze, J.; Schmuki, P. Phase Composition, Size, Orientation, and Antenna Effects of Self-Assembled Anodized Titania Nanotube Arrays: A Polarized Micro-Raman Investigation. *J. Phys. Chem. C* **2008**, *112*, 20574.
(31) Crawford, G. A.; Chawla, N. Tailoring TiO_2 Nanotube Growth During Anodic Oxidation by Crystallographic Orientation of Ti. *Scr. Mater.* **2009**, *60*, 874−877.

DOI: 10.1021/am507181p
ACS Appl. Mater. Interfaces 2015, 7, 1662−1668